

PERFORMANCE EVALUATION OF SLIDING MODE CONTROL FOR INDUCTION MOTOR BASED ON FUZZY LUENBERGER OBSERVER AND KALMAN FILTER

A. Bennassar, M. Barara, A. Abbou, M. Akherraz

Department of Electrical Engineering
Mohammed V University, Mohammadia School of Engineers, Rabat, Morocco.
ab.bennassar@gmail.com

Abstract: In this paper, a fuzzy Luenberger observer (LO) and a Kalman filter (KF) are combined for sensorless sliding mode control (SMC) of induction motor drives (IM). The rotor speed and flux are estimated by using the fuzzy LO and the KF respectively. The sliding mode control technique utilizes a robust control law to model uncertain and disturbances while the system in sliding mode. We use a saturation function to limit phenomenon chattering that presents the major problem to variable structure system (VSS). Simulation results are included to illustrate the performance and the robustness of the proposed control scheme in high and low speeds.

Key words: Luenberger observer, Kalman filter, sliding mode control, fuzzy logic, induction motor, chattering phenomenon, variable structure system.

1. Introduction

The induction motor is one of the most widely used machines in various industrial applications due to its high reliability, relatively low cost, and modest maintenance requirements. Several methods of control are used to control the induction motor among which the field orientation control that allows a decoupling between the flux and the torque, in order to obtain an independent control of the flux and the torque like dc motors [1]. Furthermore, the control of dynamical systems in presence of uncertain and disturbances is a common problem when algorithms of classical regulation such as proportional-integral controllers are used. The effect of these uncertainties on the system dynamics should be carefully taken into account in the controller design phase since they can worsen the performance or even cause system instability [2]. For this reason, several tools are proposed in the literature, from which we quote the variable structure system (VSS) [3].

The sliding mode control is a type of variable structure system characterized by high simplicity and robustness against insensitivity to parameters variation and disturbances. This approach utilizes discontinuous control laws to drive the system state trajectory into a sliding or switching surface in the state space. However, the discontinuous control presents a major drawback and constitutes the main criticism to the sliding mode control techniques. To reduce indeed limit this problem, a saturation function is used in design of sliding mode controllers.

The sensorless speed control of induction motor drives has received over the last few years a great interest. Thus it is necessary to eliminate the speed sensor to reduce hardware and increase mechanical robustness. The main techniques of sensorless control of induction motors are: Model reference adaptive systems (MRAS), Kalman filter (KF) [4] and Luenberger observer (LO) [5]. In this work, a Luenberger observer, with fuzzy adaptation mechanism combined with a Kalman filter are used simultaneously for the estimation of the rotor speed and flux respectively of induction motor drives.

2. Induction motor model

The dynamic model of the induction motor written in (d-q) reference frame can be described by the state equation as follows [6]:

$$\begin{cases} \dot{x} = Ax + Bu \\ y = Cx \end{cases} \quad (1)$$

Where x is the state vector of the system, u is the control vector and y is the output vector given as:

$$x = \begin{bmatrix} i_{sd} & i_{sq} & \phi_{rd} & \phi_{rq} \end{bmatrix}^t; u = \begin{bmatrix} u_{sd} & u_{sq} \end{bmatrix}^t; y = \begin{bmatrix} i_{sd} & i_{sq} \end{bmatrix}^t$$

A , B and C are matrices given by:

$$A = \begin{bmatrix} -\gamma & \omega_s & \frac{\mu}{T_r} & \mu\omega \\ -\omega_s & -\gamma & -\mu\omega & \frac{\mu}{T_r} \\ \frac{M}{T_r} & 0 & -\frac{1}{T_r} & \omega_r \\ 0 & \frac{M}{T_r} & -\omega_r & \frac{1}{T_r} \end{bmatrix}; B = \begin{bmatrix} \frac{1}{\sigma L_s} & 0 \\ 0 & \frac{1}{\sigma L_s} \\ 0 & 0 \\ 0 & 0 \end{bmatrix}$$

$$C = \begin{bmatrix} 1 & 0 & 0 & 0 \\ 0 & 1 & 0 & 0 \end{bmatrix}$$

With:

$$\gamma = \left(\frac{R_s}{\sigma L_s} + \frac{1-\sigma}{\sigma T_r} \right); \mu = \frac{M}{\sigma L_s L_r}; \sigma = 1 - \frac{M^2}{L_s L_r}; T_r = \frac{L_r}{R_r}$$

3. Direct field oriented control

The vector control of induction motor technique imposes the orientation of the rotor flux with respect to the d-axis, $\varphi_{rd} = \varphi_r$ and $\varphi_{rq} = 0$. In these conditions, the model of the induction motor is written by the following equations system:

$$\begin{cases} \frac{di_{sd}}{dt} = -\gamma i_{sd} + \omega_s i_{sq} + \frac{\mu}{T_r} \varphi_r + \frac{1}{\sigma L_s} v_{sd} \\ \frac{di_{sq}}{dt} = -\gamma i_{sq} - \omega_s i_{sd} - \mu \varphi_r \omega + \frac{1}{\sigma L_s} v_{sq} \\ \frac{d\varphi_{rd}}{dt} = \frac{M}{T_r} i_{sd} - \frac{1}{T_r} \varphi_r \\ \frac{d\varphi_{rq}}{dt} = \frac{M}{T_r} i_{sq} - (\omega_s - \omega) \varphi_r \\ \frac{d\Omega}{dt} = \frac{PM}{JL_r} \varphi_r i_{sd} - \frac{f}{J} \Omega - \frac{T_L}{J} \end{cases} \quad (2)$$

The space angle of the rotor flux is given by the following equation:

$$\theta_s = \int \omega_s dt ; \quad \omega_s = \omega_r + \omega \quad (3)$$

With ω_r is the slip angular speed:

$$\omega_r = \frac{Mi_{sq}}{T_r \varphi_r} \quad (4)$$

4. Sliding mode control

Sliding mode technique is a type of variable structure system (VSS) applied to the non-linear systems. The sliding mode control design is to force the system state trajectories to the sliding surface $S(x)$ and to stay on it by means a control defined by the following equation [7]:

$$u = u_{eq} + u_n \quad (5)$$

Where u_{eq} and u_n represent the equivalent control and the discontinue control respectively.

$$u_n = k \cdot \text{sat} \left(\frac{s}{\xi} \right) \quad (6)$$

Here ξ defines the thickness of the boundary layer and

$\text{sat} \left(\frac{s}{\xi} \right)$ is a saturation function.

$$\text{sat} \left(\frac{s}{\xi} \right) = \begin{cases} \text{sgn} \left(\frac{s}{\xi} \right) si \left| \frac{s}{\xi} \right| > 1 \\ \frac{s}{\xi} & si \left| \frac{s}{\xi} \right| < 1 \end{cases} \quad (7)$$

To attract the trajectory of the system towards the sliding surface in a finite time, $u_n(x)$ should be chosen such that Lyapunov function satisfies the Lyapunov stability:

$$\dot{S}(x) S(x) < 0 \quad (8)$$

The general equation to determine the sliding surface proposed is as follow [8]:

$$S(x) = \left(\frac{d}{dt} + \lambda \right)^{n-1} e \quad (9)$$

Here, e is the tracking error vector, λ is a positive coefficient and n is the system order.

4.1 Design of speed controller

Considering the equation (9) and taken $n=1$, the sliding surface of speed can be defined as:

$$S(\Omega) = \Omega^* - \Omega \quad (10)$$

By derivation of equation (10) and taken the fifth equation of the system (2), we obtain:

$$\dot{S}(\Omega) = \dot{\Omega}^* - \frac{PM}{JL_r} \varphi_{rd} i_{sq} - \frac{T_L}{J} - \frac{f}{J} \Omega \quad (11)$$

We take:

$$i_{sq} = i_{sq}^{eq} + i_{sq}^n \quad (12)$$

During the sliding mode and in permanent regime, $S(\Omega) = \dot{S}(\Omega) = 0$, $i_{sq}^n = 0$. The equivalent control action can be defined as follow:

$$i_{sq}^{eq} = \frac{JL_r}{PM \varphi_{rd}} \left(\Omega^* + \frac{T_L}{J} + \frac{f}{J} \Omega \right) \quad (13)$$

During the convergence mode, the condition $\dot{S}(\Omega) S(\Omega) < 0$ must be verified. Therefore, the discontinue control action can be given as:

$$i_{sq}^n = k_{isq} \text{sat} \left(\frac{S(\Omega)}{\xi_{isq}} \right) \quad (14)$$

To verify the system stability, coefficient k_{isq} must be strictly positive.

4.2 Design of flux controller

Considering the equation (9) and taken $n=1$, the sliding surface of flux can be defined as:

$$S(\varphi_{rd}) = \varphi_{rd}^* - \varphi_{rd} \quad (15)$$

By derivation of equation (15) and taken the third equation of the system (2), we obtain:

$$\dot{S}(\varphi_{rd}) = \dot{\varphi}_{rd}^* + \frac{1}{T_r} \varphi_{rd} i_{sq} - \frac{M}{T_r} i_{sd} \quad (16)$$

We take:

$$i_{sd} = i_{sd}^{eq} + i_{sd}^n \quad (17)$$

During the sliding mode and in permanent regime, $S(\varphi_{rd}) = \dot{S}(\varphi_{rd}) = 0$, $i_{sd}^n = 0$. The equivalent control action can be defined as follow:

$$i_{sd}^{eq} = \frac{L_r}{M} \left(\dot{\varphi}_{rd}^* + \frac{1}{T_r} \varphi_{rd} \right) \quad (18)$$

During the convergence mode, the condition $\dot{S}(\varphi_{rd})S(\varphi_{rd}) < 0$ must be verified. Therefore, the discontinue control action can be given as:

$$i_{sd}^n = k_{isd} \cdot \text{sat} \left(\frac{S(\varphi_{rd})}{\xi_{isd}} \right) \quad (19)$$

To verify the system stability, coefficient k_{isd} must be strictly positive.

4.3 Design of current controllers

Considering the equation (9) and taken $n=1$, the sliding surface of stator currents can be defined as:

$$S(i_{sd}) = i_{sd}^* - i_{sd} \quad (20)$$

$$S(i_{sq}) = i_{sq}^* - i_{sq} \quad (21)$$

By derivation of equation (20) and (21) and taken the first and second equation of the system (2) respectively, we obtain:

$$\dot{S}(i_{sd}) = \dot{i}_{sd}^* + \gamma i_{sd} - \omega_s i_{sq} - \frac{\mu}{T_r} \varphi_r - \frac{1}{\sigma L_s} v_{sd} \quad (22)$$

$$\dot{S}(i_{sq}) = \dot{i}_{sq}^* + \gamma i_{sq} + \omega_s i_{sd} + \mu \varphi_r \omega - \frac{1}{\sigma L_s} v_{sq} \quad (23)$$

During the sliding mode, $S(i_{sd}) = \dot{S}(i_{sd}) = 0$, $v_{sd}^n = 0$ and $S(i_{sq}) = \dot{S}(i_{sq}) = 0$, $v_{sq}^n = 0$. The equivalent control actions can be defined as follow:

$$v_{sd}^{eq} = \sigma L_s \left(\dot{i}_{sd}^* + \gamma i_{sd} - \omega_s i_{sq} - \frac{\mu}{T_r} \varphi_r \right) \quad (24)$$

$$v_{sq}^{eq} = \sigma L_s \left(\dot{i}_{sq}^* + \gamma i_{sq} + \omega_s i_{sd} + \mu \omega \varphi_r \right) \quad (25)$$

During the convergence mode, the conditions $\dot{S}(i_{sd})S(i_{sd}) < 0$ and $\dot{S}(i_{sq})S(i_{sq}) < 0$ must be verified. Therefore, the discontinue control action can be given as:

$$v_{sd}^n = k_{vsd} \cdot \text{sat} \left(\frac{S(i_{sd})}{\xi_{vsd}} \right) \quad (26)$$

$$v_{sq}^n = k_{vsq} \cdot \text{sat} \left(\frac{S(i_{sq})}{\xi_{vsq}} \right) \quad (27)$$

To verify the system stability, coefficients k_{vsd} and k_{vsq} must be strictly positive.

5. Fuzzy logic controller

Figure 1 shows the block diagram of fuzzy logic controller system where the variables K_p , K_i and B are used to tune the controller.

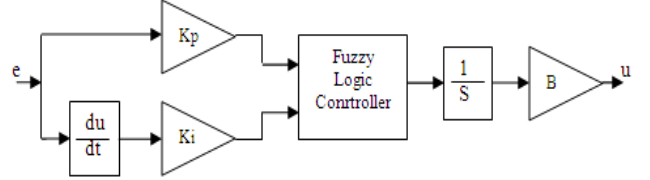


Fig. 1. Block diagram of fuzzy logic controller

There are two inputs, the error e and the change of error ce . The FLC consists of four major blocks, fuzzification, knowledge base, inference engine and defuzzification.

5.1 Fuzzification

The input variables e and ce are transformed into fuzzy variables referred to as linguistic labels. The membership functions associated to each label have been chosen with triangular shapes. The following fuzzy sets are used, NL (Negative Large), NM (Negative Medium), NS (Negative Small), ZE (Zero), PS (Positive Small), PM (positive Medium), and PL (Positive Large). The universe of discourse is set between -1 and 1 . The membership functions of these variables are shown in Figure 2.

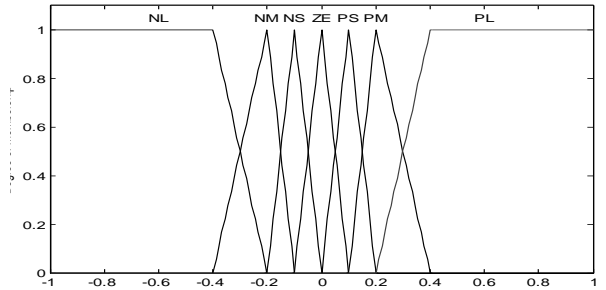


Fig. 2. Membership functions

5.2 Knowledge base and inference engine

The knowledge base consists of the data base and the rule base. The data base provides the information which is used to define the linguistic control rules and the fuzzy data in the fuzzy logic controller. The rule base specifies the control goal actions by means of a set of linguistic control rules [9]. The inference engine evaluates the set of IF-THEN and executes 7×7 rules as shown in Table 1.

Table 1

Fuzzy rules base

ce/e	NL	NM	NS	ZE	PS	PM	PL
NL	NL	NL	NL	NL	NM	NS	ZE
NM	NL	NL	NL	NM	NS	ZE	PS
NS	NL	NL	NM	NS	ZE	PS	PM
ZE	NL	NM	NS	ZE	PS	PM	PL
PS	NM	NS	ZE	PS	PM	PL	PL
PM	NS	ZE	PS	PM	PL	PL	PL
PL	ZE	PS	PM	PL	PL	PL	PL

5.3 Defuzzification

In this stage, the fuzzy variables are converted into crisp variables. There are many defuzzification techniques to produce the fuzzy set value for the output fuzzy variable. In this paper, the centre of gravity defuzzification method is adopted here and the inference strategy used in this system is the Mamdani algorithm.

6. Speed estimation with Luenberger observer

The Luenberger observer is a deterministic type of observer based on a deterministic model of the system [10] and does not take account the presence of the noises. In this work, the Luenberger observer with fuzzy adaptation mechanism is used to estimate the rotor speed of induction motor. In general, the equations of the LO can be expressed as follow:

$$\begin{cases} \dot{\hat{x}} = A\hat{x} + Bu + L(y - \hat{y}) \\ \hat{y} = C\hat{x} \end{cases} \quad (28)$$

The symbol $\hat{\cdot}$ denotes estimated value and L is the observer gain matrix. The estimation error of the stator current and rotor flux, which is the difference between the observer and the model of the motor, is given by [11]:

$$\dot{e} = (A - LC)e + \Delta A\hat{x} \quad (29)$$

Where:

$$e = x - \hat{x} \quad (30)$$

$$\Delta A = A - \hat{A} = \begin{bmatrix} 0 & 0 & 0 & \mu\Delta\omega \\ 0 & 0 & -\mu\Delta\omega & 0 \\ 0 & 0 & 0 & -\Delta\omega \\ 0 & 0 & \Delta\omega_r & 0 \end{bmatrix} \quad (31)$$

$$\Delta\omega = \omega - \hat{\omega} \quad (32)$$

We consider the following Lyapunov function defined by:

$$V = e^T e + \frac{(\Delta\omega)^2}{\lambda} \quad (33)$$

Where λ is a positive parameter. Its derivative is given as:

$$\dot{V} = e^T \left\{ (\dot{A} - LC)^T + (A - LC) \right\} e - 2\mu\Delta\omega(e_{is\alpha}\hat{\varphi}_{r\beta} - e_{is\beta}\hat{\varphi}_{r\alpha}) + \frac{2}{\lambda}\Delta\omega\dot{\omega} \quad (34)$$

The adaptation law for the estimation of the rotor speed can be deduced by the equality between the second and third terms of (34):

$$\dot{\omega} = \int \lambda\mu(e_{is\alpha}\hat{\varphi}_{r\beta} - e_{is\beta}\hat{\varphi}_{r\alpha})dt \quad (35)$$

The speed is estimated by a PI controller described as:

$$\hat{\omega} = K_p(e_{is\alpha}\hat{\varphi}_{r\beta} - e_{is\beta}\hat{\varphi}_{r\alpha}) + \frac{K_i}{s} \int (e_{is\alpha}\hat{\varphi}_{r\beta} - e_{is\beta}\hat{\varphi}_{r\alpha})dt \quad (36)$$

With K_p and K_i are positive constants. The feedback gain matrix L is chosen to ensure the fast and robust dynamic performance of the closed loop observer [12, 13].

$$L = \begin{bmatrix} l_1 & -l_2 \\ l_2 & l_1 \\ l_3 & -l_4 \\ l_4 & l_3 \end{bmatrix} \quad (37)$$

With l_1, l_2, l_3 and l_4 are given by:

$$l_1 = (d-1)\left(\gamma + \frac{1}{T_r}\right)$$

$$l_2 = -(d-1)\hat{\omega}$$

$$l_3 = \frac{(d^2-1)}{\mu}\left(\gamma - \mu\frac{M}{T_r}\right) + \frac{(d-1)}{\mu}\left(\gamma + \frac{1}{T_r}\right)$$

$$l_4 = -\frac{(d-1)}{\mu}\hat{\omega}$$

Where d is a positive coefficient obtained by pole placement approach [14]. In this work, we will replace the PI controller in LO adaptation mechanism by a fuzzy logic controller as shown in the following figure.

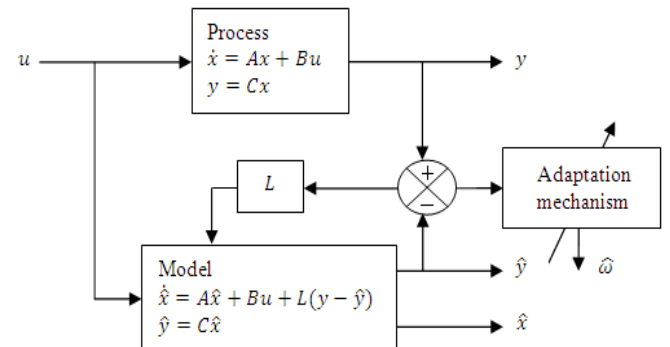


Fig. 3. Block diagram of fuzzy Luenberger observer

7. Flux estimation with Kalman filter

The Kalman filter can be used to estimate state and parameters for nonlinear systems. In this work, we estimate the rotor flux of induction motor by using KF.

Considering the process noise w and the measurement noise v , the dynamic behavior of the induction motor can be given by the following system [15, 16]:

$$\dot{x} = f(x, u) + w \quad (38)$$

$$y = h(x) + v \quad (39)$$

Where:

$$f(x, u) = \begin{bmatrix} -\gamma i_{sa} + \frac{\mu}{T_r} \phi_{ra} + \mu \omega \phi_{r\beta} + \frac{1}{\sigma L_s} u_{sa} \\ -\gamma i_{s\beta} - \mu \omega \phi_{ra} + \frac{\mu}{T_r} \phi_{r\beta} + \frac{1}{\sigma L_s} u_{s\beta} \\ \frac{M}{T_r} i_{sa} - \frac{1}{T_r} \phi_{ra} - \omega \phi_{r\beta} \\ \frac{M}{T_r} i_{s\beta} + \omega \phi_{ra} - \frac{1}{T_r} \phi_{r\beta} \end{bmatrix}$$

$$h(x) = [i_{sa} \ i_{s\beta}]^T$$

The covariance matrices Q and R of these noises are defined respectively as:

$$Q = \text{cov}(w) = E\{ww^t\}; R = \text{cov}(v) = E\{vv^t\}$$

From the induction motor dynamic model, the rotor flux can be estimated by the following Kalman filter algorithm.

1) Prediction of state variables :

$$\hat{x}_{k+1|k} = f(x_{k|k}, u_k) \quad (40)$$

2) Estimation of error covariance matrix :

$$P_{k+1|k} = F_k P_{k|k} F_k^t + Q \quad (41)$$

Where:

$$F_k = \left. \frac{\partial f(x_{k|k}, u_k)}{\partial x_k} \right|_{x_k = \hat{x}_{k|k}} \quad (42)$$

$$F_k = \begin{bmatrix} 1 - T_s \gamma & 0 & T_s \frac{\mu}{T_r} & T_s \mu \omega \\ 0 & 1 - T_s \gamma & -T_s \mu \omega & T_s \frac{\mu}{T_r} \\ T_s \frac{M}{T_r} & 0 & 1 - T_s \frac{1}{T_r} & -T_s \omega \\ 0 & T_s \frac{M}{T_r} & T_s \omega & 1 - T_s \frac{1}{T_r} \end{bmatrix}$$

3) Kalman filter gain :

$$K_{k+1} = P_{k+1|k} H_k^t [H_k P_{k+1|k} H_k^t + R]^{-1} \quad (43)$$

Where:

$$H_k = \left. \frac{\partial h(x_k)}{\partial x_k} \right|_{x_k = \hat{x}_{k|k}} \quad (44)$$

$$H_k = \begin{bmatrix} 1 & 0 & 0 & 0 \\ 0 & 1 & 0 & 0 \end{bmatrix}$$

4) Estimation of state variables :

$$\hat{x}_{k+1|k+1} = \hat{x}_{k+1|k} + K_{k+1} (y_{k+1} - H_k \hat{x}_{k+1|k}) \quad (45)$$

5) Update of error covariance matrix :

$$P_{k+1|k+1} = P_{k+1|k} - K_{k+1} H_k P_{k+1|k} \quad (46)$$

Figure 4 shows the block diagram of the proposed control scheme for sensorless sliding mode control for field oriented control of induction motor.

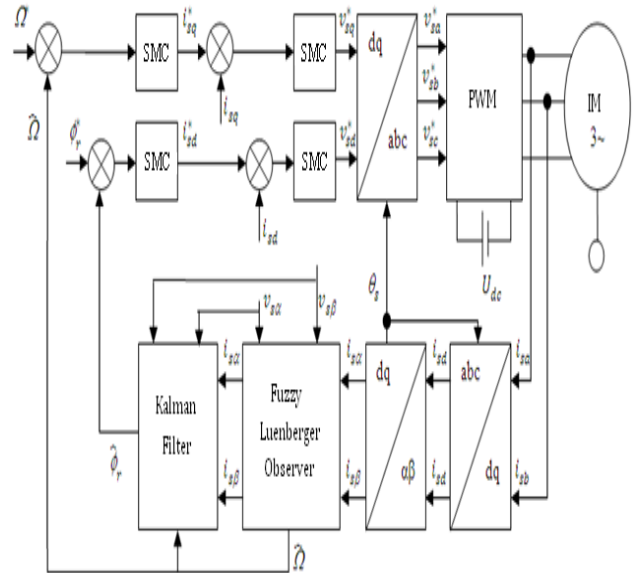


Fig. 4. Block diagram for sensorless sliding mode control of induction motor

8. Simulation results and discussion

A series of simulation tests were carried out on sliding mode control of induction motor using Luenberger observer combined with Kalman filter. Simulations have been realized under the Matlab/Simulink environment.

The parameters of the induction motor are given in Appendix. Many cases are considered in the following simulation tests.

8.1 Operating with no and full load

The rotor flux reference is fixed to 1 Wb and the speed reference value is set to 100 rad/s. A load torque with 10 N.m is applied at $t=1$ s and eliminated at $t=2$ s.

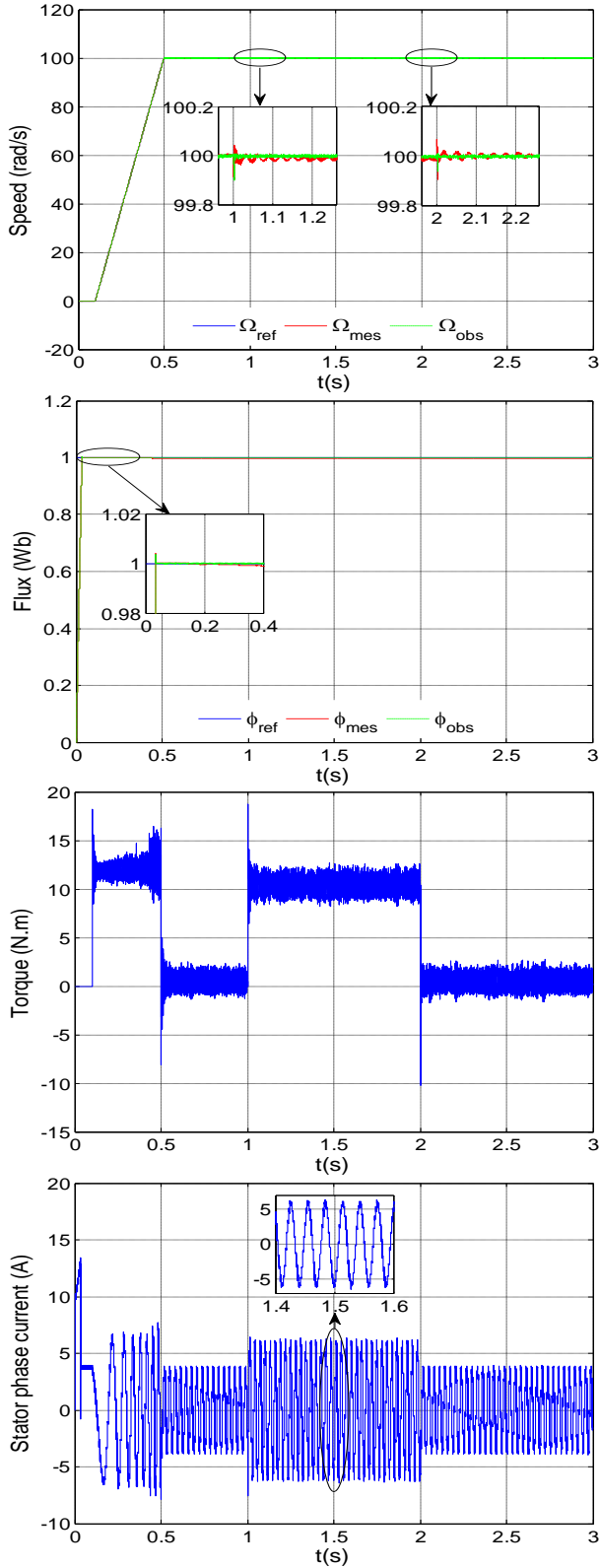


Fig. 5. Simulation responses under load torque

8.2 Operating with reverse speed rotation

In this case, a test of robustness of the control is realized by the reverse speed rotation between -100 rad/s and 100 rad/s.

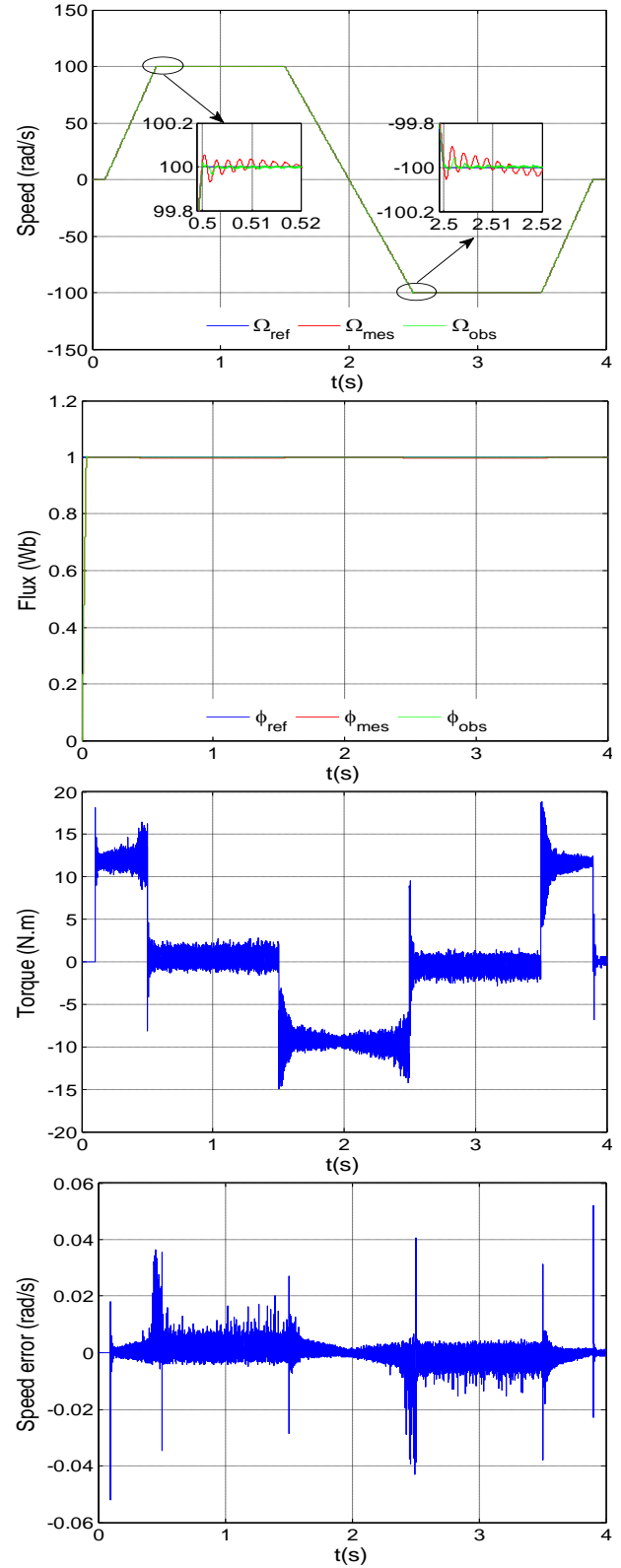


Fig. 6. Simulation responses with reverse speed

8.3 Operating with low speed functioning

In this case, the estimated speed is carried out for low speed between -10 rad/s and 10 rad/s and we set the rotor flux to 1 Wb.

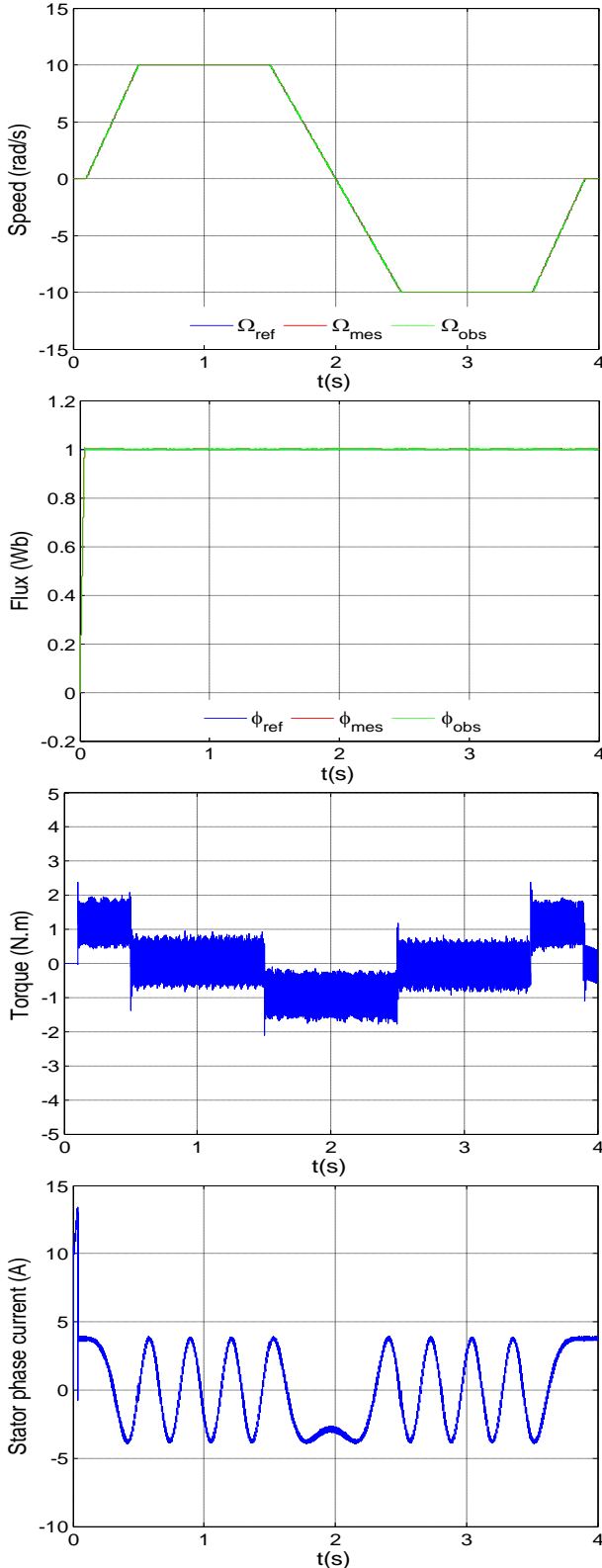


Fig. 7. Simulation responses at low speed

With the simulation results illustrated in figures 5, 6 and 7, we can notice the good estimated speed tracking performance test in different working during application of load torque, reverse speed rotation and low speed operation in terms of overshoot, static error and fast response. The estimation error is near to zero. The observed flux is similar to the nominal case during application of the load. The stator phase current remains sinusoidal and takes appropriate value.

It is evident from these simulation results that the proposed sliding mode controllers of induction motor drives present an excellent performance and robustness and the new observer gives the better results.

9. Conclusion

In this research, we have investigated the sliding mode controllers designed to achieve thrust, flux and speed tracking objective under load torque disturbance associated to the Luenberger observer and Kalman filter for sensorless induction motor drives control. The numerical simulation has shown that this nonlinear control and combining observation techniques ensure good performance and allow a complete decoupling between the flux and the torque and guarantee a good robustness towards load torque disturbance.

Appendix

Table 2
Induction motor parameters

Rated power	3 KW
Voltage	380V Y
Frequency	50 Hz
Pair pole	2
Rated speed	1440 rpm
Stator resistance	2.2 Ω
Rotor resistance	2.68 Ω
Stator inductance	0.229 H
Rotor inductance	0.229 H
Mutual inductance	0.217 H
Moment of inertia	0.047 kg.m ²
Viscous friction	0.004 N.m.s/rad

References

1. Blaschke, F.: *The principle of field orientation as applied to the new transvector closed loop control system for rotating-field machines*, Siemens Rev, 4, 1972, p. 217–220.
2. Vecchio, V.: *Sliding Mode Control: Theoretical Development and Applications to uncertain mechanical system*, Universita Degli Studi Pavia.
3. Bennassar, A., Abbou, A., Akherraz, M., Barara, M.: *A new sensorless control design of induction motor based on backstepping sliding mode approach*, International Review on Modelling and Simulations, Vol. 7, No. 1, 2014, p. 35-42.

4. Morino, R., and Tomei, P.: *Nonlinear control design adaptive and robust*, Prentice-Hall, 1995.
5. Luenberger, D-G. : *Observing the state of a linear system*, IEEE Transactions on Industrial Electronics, MLI-8, 1964.
6. Caron, J.P., Hautir, J.P.: *Modélisation et commande de la machine asynchrone*, Editions Technip, Paris, 1995.
7. Utkin, V.I.: *Variable Structure System with Sliding Modes*, IEEE Transactions Automatic and Control, AC-22, 1993, p. 212-221.
8. Slotine, J.J.E., Li, W.: *Applied Nonlinear Control*, Prentice-Hall. Inc, 1991.
9. Peter, V.: *Sensorless Vector and Direct Torque Control*, Oxford New, York Tokyo, Oxford University Press, 1998.
10. Gacho, J., Zalman, M.: *IM based speed servodrive with luenberger observer*, Journal of Electrical Engineering, Vol. 6, No. 3, 2010, p. 149-156.
11. Maes, J., Melkebeek, J.: *Speed sensorless direct torque control of induction motor using an adaptive flux observer*, *Proc. Of IEEE Transactions on Industry Applications*, Vol. 36, 2000, p. 778-785.
12. Belkacem, S., Naceri, F., Betta, A., Laggoune, L.: *Speed sensorless of induction motor based on an improved adaptive flux observer*, IEEE Transactions Industry Applications, 2005, p. 1192-1197.
13. Akin, B.: *State estimation techniques for speed sensorless field orient control of induction motors*, M.Sc. Thesis EE Dept, METU, 2003.
14. Sio-Iong Ao Len Gelman: *Advances in Electrical Engineering and Computational Science Lecture*, Notes in Electrical Engineering, Vol. 39, Editors, 2009.
15. Kim, Y.R., Sul, S.K., Park, M.H.: *Speed sensorless vector control of induction motor, using extended Kalman filter*, IEEE Transactions on Industry Applications, Vol. 30, No. 5, 1994, p. 1225-1233.
16. Shi, K.L., Chan, T.F., Wong, Y.K., Ho, S.L.: *Speed estimation of an induction motor drive using an optimized extended Kalman filter*, IEEE Transactions on Industrial Electronics, Vol. 49, 2002, p. 124-133.
17. Bennisar, A., Abbou, A., Akherraz, M.: *Speed sensorless indirect field oriented control of induction motor using an extended Kalman filter*, Journal of Electrical Engineering, Vol. 13, No. 1, 2013, p. 238-243.
18. Young-Real Kim, Seung-Ki Sul, and Min-Ho Park. : *Speed sensorless vector control of induction motor using extended Kalman filter*, IEEE Transactions on Industry Applications, Vol. 30, No. 5, 1994, p. 1225-1233.
19. Iwasaki, T., and Kataoka, T. : *Application of an extended Kalman filter to parameter identification of an induction motor*, IEEE US Annu. Meet. Conf. Rec., 1989, p. 248-253.
20. Zai, C.L., and Lipo, T.A. : *An extended Kalman filter approach to rotor time constant measurcment in PWM induction motor drives*, IEEE LAS Annu. Meet. Conf. Rec., 1987, p. 177-183.